J|A|C|S
ARTICLES
Published on Web 03/10/2005

Evolution of Fluorescein as a Platform for Finely Tunable Fluorescence Probes

Yasuteru Urano,*,†,‡ Mako Kamiya,† Kojiro Kanda,† Tasuku Ueno,† Kenzo Hirose,§ and Tetsuo Nagano*,†

Contribution from the Graduate Schools of Pharmaceutical Sciences and of Medicine, The University of Tokyo, Hongo, Bunkyo-ku, Tokyo 113-0033, and PRESTO, JST Agency, Honcho, Kawaguchi-shi, Saitama 332-0012, Japan

Received October 6, 2004; E-mail: urano@mol.f.u-tokyo.ac.jp; tlong@mol.f.u-tokyo.ac.jp

Abstract: Fluorescence imaging is the most powerful technique currently available for continuous observation of dynamic intracellular processes in living cells. Suitable fluorescence probes are naturally of critical importance for fluorescence imaging, but only a very limited range of biomolecules can currently be visualized because of the lack of flexible design strategies for fluorescence probes. At present, design is largely empirical. Here we show that the carboxylic group of traditional fluorescein dyes, formerly considered indispensable, has been replaced with other substituents, affording various kinds of new fluoresceins. Further, by breaking out of the traditional structure of fluorescein, we developed the first and totally rational design strategy for novel fluorescence probes based on a strict photochemical basis. The value of this approach is exemplified by its application to develop a novel, highly sensitive, and membrane-permeable fluorescence probe for β-galactosidase, which is the most widely used reporter enzyme.

Introduction

Fluorescence probes are excellent sensors for biomolecules, being sensitive, fast-responding, and capable of affording high spatial resolution via microscopic imaging.[1] Suitable fluorescence probes are naturally of critical importance for fluorescence imaging,[2,3] but only a very limited range of biomolecules can currently be visualized because of the lack of flexible design strategies for fluorescence probes. At present, design is largely empirical.

Fluorescein was first developed in the 19th century,[4] and has become widely known as a highly fluorescent molecule that emits longer wavelength light upon excitation at around 500 nm in aqueous media.[5,6] Fluorescein derivatives have been used as fluorescent tags for many biological molecules such as protein, DNA, and so on, as well as a platform for many kinds of fluorescence probes. For example, fluo-3 is a dichlorofluorescein probe for Ca^{2+} (*3*). Recently, we have developed a range of novel fluorescein-based fluorescence probes.[7−11] All these probes are almost nonfluorescent before reaction or binding with target molecules, but become highly fluorescent after reaction or binding.

Initially, the mechanism underlying the fluorescence off/on switching of fluorescein derivatives was unclear, because only limited empirical information was available about the fluorescence properties of fluorescein derivatives.[12] Recently, we demonstrated that the fluorescein molecule could be understood as a directly linked donor−acceptor system, in that photoinduced electron transfer (PeT) might determine its quantum efficiencies of fluorescence (Φ_{fl}).[13] PeT is a well-known mechanism through which the fluorescence of a fluorophore is quenched by electron transfer from the donor to the acceptor fluorophore.[2,14] Although there is no obvious linker within the fluorescein molecule, our study strictly revealed that the benzoic acid moiety of weakly fluorescent fluoresceins could be an electron donor to the excited fluorophore 6-hydroxy-3*H*-xanthen-3-one, because these two moieties were orthogonal to each other and there was no ground-state interaction between them.

We next focused on the role of the carboxylic group of fluorescein. Almost all currently known fluorescein derivatives contain the carboxylic group. Further, Lindqvist et al. reported

† Graduate School of Pharmaceutical Sciences, The University of Tokyo.
‡ PRESTO, JST Agency.
§ Graduate School of Medicine, The University of Tokyo.

(1) Tsien, R. Y. In *Fluorescent and Photochemical Probes of Dynamic Biochemical Signals Inside Living Cells*; Czarnik, A. W., Ed.; American Chemical Society: Washington, DC, 1993; pp 130−146.
(2) de Silva, A. P.; Gunaratne, H. Q. N.; Gunnlaugsson, T.; Huxley, A. J. M.; McCoy. C. P.; Rademacher, J. T.; Rice, T. E. *Chem. Rev.* **1997**, *97*, 1515−1566.
(3) Minta, A.; Kao, J. P. Y.; Tsien, R. Y. *J. Biol. Chem.* **1989**, *264*, 8171−8178.
(4) Baeyer, A. *Ber. Dtsch. Chem. Ges.* **1871**, *4*, 555−558.
(5) Weber, G.; Teale, F. W. J. *Trans. Faraday Soc.* **1958**, *54*, 640−648.
(6) Paeker, C. A.; Rees, W. T. *Analyst* **1960**, *85*, 587−600.
(7) Tanaka, K.; Miura, T.; Umezawa, N.; Urano, Y.; Kikuchi, K.; Higuchi, T.; Nagano, T. *J. Am. Chem. Soc.* **2001**, *123*, 2530−2536.
(8) Kojima, H.; Nakatsubo, N.; Kikuchi, K.; Kawahara, S.; Kirino, Y.; Nagoshi, H.; Hirata, Y.; Nagano, T. *Anal. Chem.* **1998**, *70*, 2446−2453.
(9) Umezawa, N.; Tanaka, K.; Urano, Y.; Kikuchi, K.; Higuchi, T.; Nagano, T. *Angew. Chem., Int. Ed.* **1999**, *38*, 2899−2901.
(10) Setsukinai, K.; Urano, Y.; Kakinuma, K.; Majima, H. J.; Nagano, T. *J. Biol. Chem.* **2003**, *278*, 3170−3175.
(11) Hirano, T.; Kikuchi, K.; Urano, Y.; Higuchi, T.; Nagano, T. *J. Am. Chem. Soc.* **2000**, *122*, 12399−12400.
(12) Munkholm, C.; Parkinson, D. R.; Walt, D. R. *J. Am. Chem. Soc.* **1990**, *112*, 2608−2612.
(13) Miura, T.; Urano, Y.; Tanaka, K.; Nagano, T.; Ohkubo, K.; Fukuzumi, S. *J. Am. Chem. Soc.* **2003**, *125*, 8666−8671.
(14) Kollmannsberger, M.; Rurack, K.; Resch-Genger, U.; Daub, J. *J. Phys. Chem. A* **1998**, *102*, 10211−10220.

10.1021/ja043919h CCC: $30.25

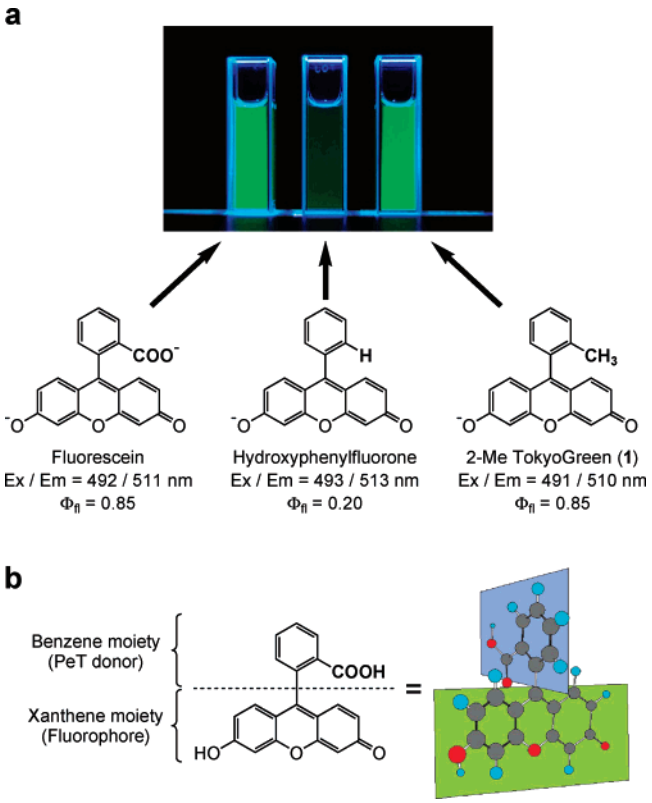

Figure 1. Breaking out of the traditional fluorescein structure by replacing the supposedly essential carboxylic group with other substituents. (a) Photos of the fluorescence of fluorescein (left), 6-hydroxy-9-phenylfluorone (middle), and our new fluorescein-based molecule (2-Me Tokyo Green (**1**), right). (b) Fluorescein structure divided into two parts, the benzene moiety and the fluorophore.

that the carboxylic group was indispensable for strong fluorescence of fluorescein, because removal of the carboxylic group caused a reduction of Φ_{fl} (Figure 1a, middle).[15,16] However, in light of our results, we developed the working hypothesis that the carboxylic group plays no role in the fluorescence properties of the fluorescein molecule, except to keep the benzene moiety and the fluorophore orthogonal to each other (Figure 1b). In other words, the carboxylic group could be replaced with another functional group.

Results and Discussion

Role of the Carboxylic Group of Fluorescein. We first synthesized a fluorescein derivative in which the carboxylic group was replaced with a methyl group. As shown in Figure 1a and Table 1, the new fluorescein, called 2-Me TokyoGreen (**1**), showed almost the same fluorescence properties as traditional fluorescein. This result clearly showed that the carboxylic group of the fluorescein molecule was *not* indispensable, but could be replaced with other substituents. Further, the fact that 2-Me TokyoGreen and fluorescein had almost identical quantum yields of fluorescence strongly suggested that even the small methyl group is sufficient to keep the benzene moiety and the fluorophore orthogonal to each other. Moreover, to our surprise, even this simple derivative (**1**) was a novel compound. This fact showed that until now very little attention has been paid to the possibility of extending the scope of the fluorescein molecule as a flexible platform for fluorescence probes by controlling its fluorescence properties in a precise manner, as we describe in this paper.

Table 1. Photophysical Properties of TokyoGreens, the Newly Developed Fluorescein Derivatives

R	excitation max[a] (nm)	emission max[a] (nm)	oxidation potential[b] (V vs SCE)	HOMO energy[c] (hartrees)	Φ_{fl} (pH 13)	Φ_{fl} (pH 3.4)
2-Me (**1**)	491	510	2.19	−0.2356	0.847	0.319
2,4-DiMe (**2**)	491	510	2.08	−0.2304	0.865	0.307
2,5-DiMe (**3**)	491	510	1.98	−0.2262	0.887	0.319
2-OMe (**4**)	494	515	1.75	−0.2174	0.860	0.076
2-Me-4-OMe (**5**)	492	509	1.66	−0.2141	0.840	0.010
2-OMe-5-Me (**6**)	494	514	1.57	−0.2098	0.500	0.004
2,4-DiOMe (**7**)	494	513	1.44	−0.2063	0.200	0.001
2,5-DiOMe (**8**)	494	512	1.26	−0.1985	0.010	0.000
fluorescein	492	511	nd[d]	−0.2646	0.85[e]	0.30[f]

[a] Measured in 0.1 N NaOH(aq). [b] Oxidation potentials of the corresponding benzene moiety. Data were obtained in acetonitrile containing 0.1 M TBAP. [c] HOMO energy level of the corresponding benzene moiety. Data were calculated with B3LYP/6-31G(d)//B3LYP/6-31G(d) by Gaussian 98W. [d] Not detectable. [e] Reference 6. [f] Reference 16.

Photophysical and Photochemical Properties of Newly Developed Fluorescein Derivatives (TokyoGreens). Next, we designed and synthesized various derivatives (TokyoGreens) whose electron density of the benzene moiety was tuned in a fine manner by introducing methyl and methoxy groups into the benzene moiety (Table 1). The fact that the absorbance and emission maxima were not altered among TokyoGreens and traditional fluorescein showed that the ground-state interaction between the benzene moiety and the xanthene moiety was minimal in all of them. On the other hand, the fluorescence quantum yield was greatly altered, depending on the oxidation potential and the HOMO energy level of the benzene moiety (Figure 2a). In the case of derivatives whose oxidation potential of the benzene moiety is higher than 1.7 V (vs SCE), very high Φ_{fl} values almost equal to the traditional fluorescein were observed in basic aqueous media. Below 1.7 V, the Φ_{fl} values dropped sharply with decreasing oxidation potential, and finally reached $\Phi_{fl} \approx 0$ in the case where the benzene moiety was *p*-dimethoxybenzene (Figure 2a, upper panel), whose oxidation potential is 1.26 V. From these results, the threshold level between fluorescence on and off lay around 1.4−1.6 V for the deprotonated anion form of xanthene, the fluorophore (Figure 2b, red line).

pH-Dependent Change of the Fluorescence on/off Threshold. In a buffered solution of pH 3.4, in which the fluorophore xanthene moiety of every derivative is protonated, the threshold level shifted to higher oxidation potential (Figure 2a, lower panel). In the case of derivatives whose oxidation potential of the benzene moiety is higher than 2.0 V, high Φ_{fl} values of around 0.3, almost equal to that of the traditional fluorescein,[16] were observed. Below 2.0 V, the Φ_{fl} values dropped sharply, and finally reached $\Phi_{fl} \approx 0$ in the case where the benzene moiety was 3-methoxytoluene (Figure 2b, blue line).

The rate of PeT could be determined from the ΔG_{PeT}, λ, and V values according to the Marcus equation.[17] All of our new fluorescein derivatives must have similar λ and V values due to their similar structures, so the major determinant should be ΔG_{PeT}, and this value could be calculated from the Rehm−

(15) Lindqvist, L.; Lundeen, G. W. *J. Chem. Phys.* **1966**, *44*, 1711−1712.
(16) Fink, D. W.; Willis, C. R. *J. Chem. Phys.* **1970**, *53*, 4720−4722.
(17) Marcus, R. A.; Eyring, H. *Annu. Rev. Phys. Chem.* **1964**, *15*, 155−196.

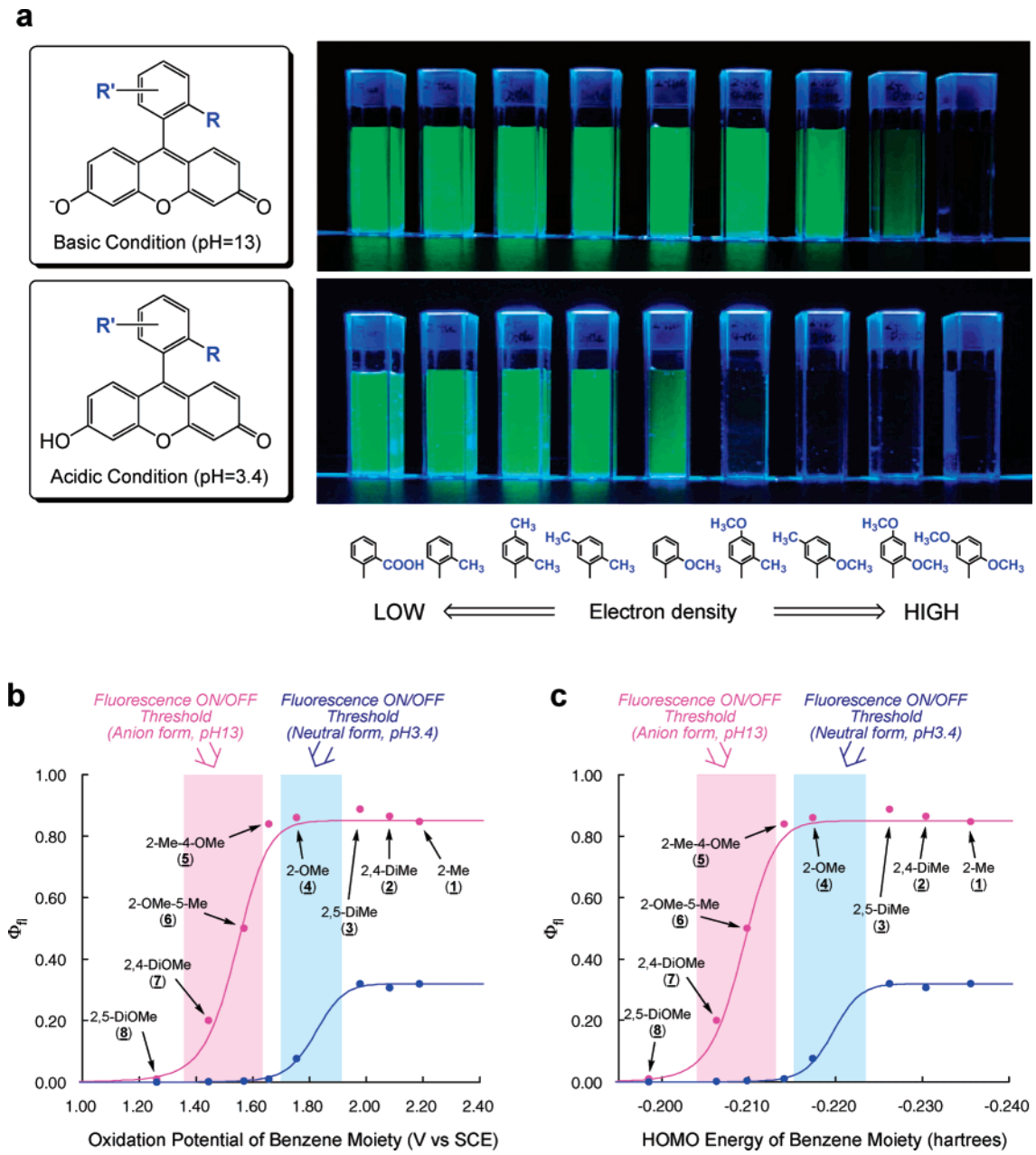

Figure 2. Dynamic changes of the quantum efficiencies of fluorescence (Φ_{fl}) of TokyoGreens, depending on the oxidation potential and the HOMO energy level of their benzene moiety. (a) Comparison of the fluorescence of TokyoGreens with a variety of benzene moieties. (b) Relationships between the oxidation potential of the benzene moiety and the Φ_{fl} of the anion form (red) and neutral form (blue) of TokyoGreens. The curves represent the best fit to the Marcus equation. (c) Relationships between the HOMO energy level of the benzene moiety and the Φ_{fl} of the anion form (red) and neutral form (blue) of TokyoGreens. The curves represent the best fit to the Marcus equation.

Weller equation,[18] $\Delta G_{PeT} = E_{ox} - E_{red} - \Delta E_{00} - w_p$, where E_{ox} and E_{red} are the oxidation and reduction potentials of the electron donor and acceptor, ΔE_{00} is the singlet excited energy, and w_p is the work term for the charge separation state. For our TokyoGreens, the xanthene moiety has the role of an electron acceptor, and it can easily be anticipated that the protonated xanthene could be more easily reduced than the deprotonated form. Indeed, the reduction potential of deprotonated fluorescein was observed as −1.21 V, and that of the protonated form was −0.78 V vs SCE in aqueous media; thus, the threshold level must be shifted to higher oxidation potential in acidic buffer. In other words, PeT would occur to the protonated xanthene fluorophore even from the more electron deficient benzene moiety.

Advantages of TokyoGreens Compared to the Traditional Fluoresceins. It is a great advantage that we can predict the Φ_{fl} of certain fluorescein derivatives without the need to synthesize them. The oxidation potential of the benzene moiety could be easily anticipated by calculating the HOMO energy levels using the density functional method with the B3LYP/6-31G(d) basis set. Indeed, the relationships between Φ_{fl} and the HOMO energy levels under basic and acidic conditions (Figure 2c) very closely matched the corresponding relationships with the oxidation potentials (Figure 2b). These findings are practically very useful for designing and developing novel fluorescence probes.

(18) Rehm, D.; Weller, A. *Isr. J. Chem.* **1970**, *8*, 259−271.

Scheme 1. Advantages in the Syntheses of TokyoGreens Compared to Those of the Traditional Fluorescein Derivatives

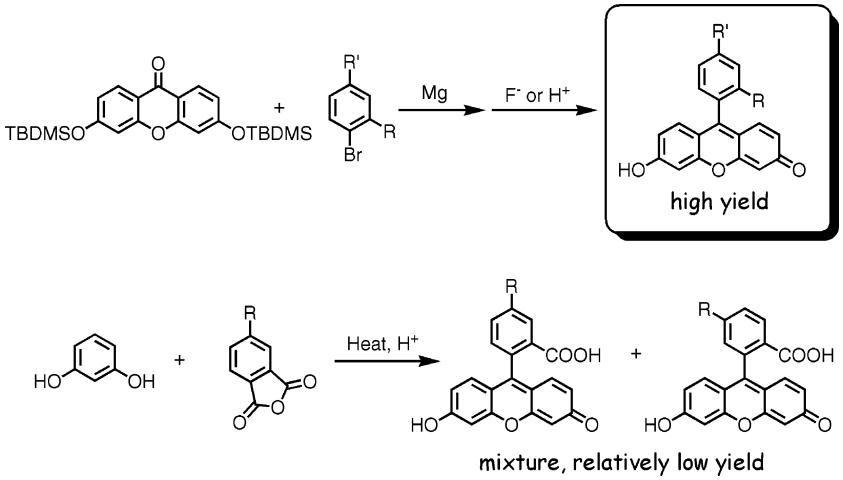

Moreover, from the synthetic point of view, our new TokyoGreens have a major advantage over traditional fluoresceins: Grignard coupling of substituted bromobenzenes and xanthone yielded a single desired isomer, in contrast to the formation of two isomers in the case of traditional fluorescein synthesis by the condensation of phthalic anhydride and resorcinol (Scheme 1).

Rational Design Strategy for Novel Fluorescence Probes and Its Application to the Development of a Novel Fluorescence Probe for *β*-Galactosidase. Our findings described above enable us to design flexibly many kinds of finely tuned fluorescence probes, on the basis of not only the change of the oxidation potential of the benzene moiety upon encounter with a target molecule, but also the change of the reduction potential of the fluorophore. Using the latter strategy, we were able to develop a novel fluorescence probe for β-galactosidase.

Glycosidases are important reporter gene markers. Among them, β-galactosidase is the most widely used gene expression marker.[19] The design strategy of our β-galactosidase probe was as follows. 2-Me-4-MeO TokyoGreen (**5**) exists mainly as an anion form under neutral to basic conditions, because the pK_a value of the xanthene fluorophore is around 6.2, and it fluoresced almost fully at neutral pH, while under acidic conditions it was almost nonfluorescent. This is because the oxidation potential of 3-methoxytoluene, which is the benzene moiety of this derivative, lies between the fluorescence on/off thresholds of the neutral and anion forms of the fluorophore (Figure 2b,c). As fluorescein *O*-methyl ether had almost the same reduction potential of -0.87 V, compared to that of the protonated xanthene fluorophore, we designed 2-Me-4-OMe TokyoGreen *O*-β-galactoside (TG-βGal) as a novel fluorescence probe for β-galactosidase (Figure 3a). Because TG-βGal has an *O*-alkylated fluorophore, 3-methoxytoluene was expected to act as a PeT donor to the xanthene moiety at neutral pH, and the Φ_{fl} value of this compound should be very small. On the other hand, β-galactosidase would mediate hydrolysis to yield **5**, which is highly fluorescent at neutral pH.

Figure 3a clearly shows that TG-βGal operates as a β-galactosidase fluorescence probe. Before the reaction, Φ_{fl} was very small and the probe was almost nonfluorescent. Upon encounter with the target β-galactosidase, hydrolysis occurred efficiently to afford highly fluorescent **5**. It should be emphasized that it is critical to keep the fluorescence of fluorescence probes as low as possible before the reaction of interest, to achieve high sensitivity, especially in live cell imaging experiments. It is usually the case that less than 1% of a fluorescence probe is converted to strongly fluorescent products in a reaction of interest, while more than 99% remains intact. Therefore, a higher background fluorescence of the fluorescence probes usually results in a poorer signal-to-noise (S/N) ratio.

This novel fluorescence probe has great advantages over the known β-galactosidase probe fluorescein di-*O*-β-galactoside (FDG).[20] First, the hydrolysis reaction of FDG occurs in two steps, while our probe has only one β-galactoside in a molecule (Figure 3a,b). Because FDG is first converted to moderately fluorescent fluorescein mono-*O*-β-galactoside (FMG), which in turn is converted to fully fluorescent fluorescein,[21,22] the relationship between the fluorescence increase and β-galactosidase activity was known to be nonlinear.[23] Moreover, the rate of fluorescence increase is very slow, and consequently, the sensitivity was relatively low (Figure 3c, inset). On the other hand, with our new TG-βGal, restoration of full fluorescence intensity requires only one step of hydrolysis, affording a higher rate of fluorescence increase and higher sensitivity, as well as ensuring strict linearity in the relationship between the fluorescence intensity and the β-galactosidase activity, as shown in Figure 3c. Further, and more significantly, our probe is membrane-permeable due to its lower hydrophilicity, and this enabled us to image β-galactosidase activity in *living* cells. So far, X-gal staining has been the most popular technique to determine whether cells express β-galactosidase or not. The X-gal technique is indeed widely used, but a cell fixation process is required. Further, FDG is well-known to be membrane-impermeable and cannot be used to take fluorescence images of living cells without a severe loading technique, such as hypotonic shock.[19] Thus, a technique which allows the real-time imaging of β-galactosidase activity in living cells has been

(19) Nolan, G. P.; Fiering, S.; Nicolas, J. F.; Herzenberg, L. A. *Proc. Natl. Acad. Sci. U.S.A.* **1988**, *85*, 2603−2607.

(20) Rotman, B.; Zderic, J. A.; Edelstein, M. *Proc. Natl. Acad. Sci. U.S.A.* **1963**, *50*, 1−6.
(21) Hofmann, J.; Sernetz, M. *Anal. Biochem.* **1983**, *131*, 180−186.
(22) Huang, Z. *Biochemistry* **1991**, *30*, 8535−8540.
(23) Fiering, S. N.; Roederer, M.; Nolan, G. P.; Micklem, D. R.; Parks, D. R.; Herzenberg, L. A. *Cytometry* **1991**, *12*, 291−301.

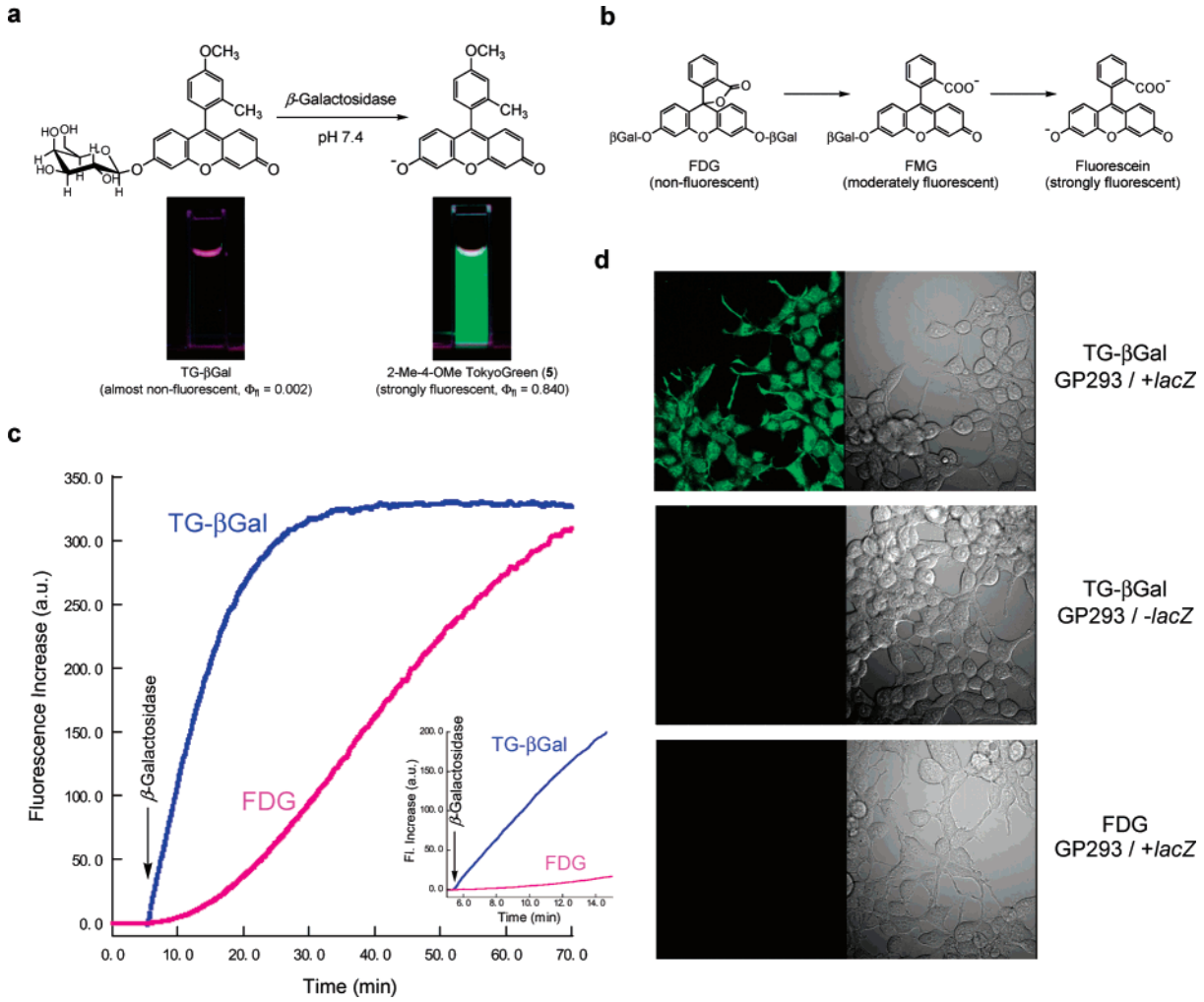

Figure 3. Development of a novel, membrane-permeable, sensitive fluorescence probe for β-galactosidase (TG-βGal). (a) Reaction scheme of TG-βGal and photos before and after the reaction with β-galactosidase. (b) Reaction scheme of fluorescein di-*O*-β-galactoside (FDG), a currently used fluorescence probe for β-galactosidase. (c) Comparison of the time course of the fluorescence increase between our TG-βGal (blue) and FDG (red) upon addition of β-galactosidase. Expansion of the initial fluorescence increase is shown in the inset. (d) Fluorescence microscopic imaging of β-galactosidase activity with TG-βGal and FDG in living *lacZ*-positive and -negative cells. The upper panel shows the images with TG-βGal in *lacZ*-positive cells, the middle panel shows those with TG-βGal in *lacZ*-negative cells, and the lower panel shows those with FDG in *lacZ*-positive cells. Fluorescence images are on the left, and bright-field images are on the right.

long awaited.[24] Figure 3d shows the application of TG-βGal and FDG to GP293 cells transduced with or without LNCX2-*lacZ* (*lacZ*-positive or *lacZ*-negative cells). We could obtain a bright image of *lacZ*(+) cells by using TG-βGal without any fixation or other complicated technique. The lower panel of Figure 3d shows the images with FDG in *lacZ*(+) cells under the same loading conditions used in the case of TG-βGal. These results clearly show the advantages of our probe for fluorescence imaging of β-galactosidase activity in living cells, as well as the value of our rational and flexible design strategy of fluorescence probes.

Conclusion

We found that the supposedly essential carboxylic group of traditional fluorescein could be replaced with other substituents, and succeeded in developing various kinds of new fluoresceins. By examining the fluorescence properties of these new fluorescein derivatives, we could determine the fluorescence on/off thresholds for both the anion and neutral forms of the xanthene fluorophore of fluorescein. We used this information to construct a practically useful strategy for designing finely tuned fluorescence probes. On the basis of this strategy, we developed a novel fluorescence probe (TG-βGal) for β-galactosidase, which has great advantages over previously known probes, especially in terms of sensitivity and for real-time imaging of living cells. We are also developing other novel fluorescence probes by utilizing this approach.

Experimental Section

Materials and General Instrumentations. General chemicals were of the best grade available, supplied by Tokyo Chemical Industries, Wako Pure Chemical, or Aldrich Chemical Co., and were used without further purification. Special chemicals consisted of dimethyl sulfoxide (DMSO; fluorometric grade, Dojindo) and tetrabutylammmonium perchlorate (TBAP; electrochemical grade, dried over P_2O_5 before use, Fluka). Acetonitrile, acetone, *N*,*N*-dimethylformamide (DMF), tetrahydrofuran (THF), methanol, and ethanol were used after appropriate distillation or purification. β-Galactosidase (molecular weight 540,000, EC 3.2.1.23) and fluorescein di-β-D-galactopyranoside (FDG) were

(24) Rowland, B.; Purkayastha, A.; Monserrat, C.; Casart, Y.; Takiff, H.; McDonough, K. A. *FEMS Microbiol. Lett.* **1999**, *179*, 317−325.

purchased from Sigma-Aldrich Japan K.K. (Tokyo, Japan). NMR spectra were recorded on a JNM-LA300 (JEOL) instrument at 300 MHz for ^{1}H NMR and 75 MHz for ^{13}C NMR. Mass spectra were measured with a JMS-DX300 (JEOL) for EI and a JMS-T100LC (JEOL) for ESI. All experiments were carried out at 298 K, unless otherwise specified.

General Procedure for the Syntheses of TokyoGreens. Xanthone diTBDMS ether was prepared according to the literature.[3] Magnesium turnings (4.50 mmol) were dried under Ar at 250 °C for 3 h. After the magnesium turnings were cooled to room temperature, 2 mL of bromobenzene derivatives (0.45 mmol) in distilled THF was added, and the mixture was stirred at 60 °C to yield phenylmagnesium bromide derivatives. The solution was cooled to 0 °C, then 2 mL of xanthone diTBDMS ether (0.30 mmol) in distilled THF was added, and the mixture was stirred for 10 min. The reaction was quenched by adding 10 mL of 2 N HCl(aq), and the resulting yellow precipitate was collected by filtration, washed with a small quantity of distilled THF, and dried in vacuo to yield almost pure product. Further purification by silica gel column chromatography was done if required.

NMR and Mass Spectral Data of TokyoGreens. 9-[1-(2-Methylphenyl)]-6-hydroxy-3*H*-xanthen-3-one (1). Yield: 96%. ^{1}H NMR (300 MHz, CD_3OD): δ 2.05 (s, 3H), 7.18 (dd, 2H, J = 2.2, 9.2 Hz), 7.29−7.32 (m, 3H), 7.47−7.64 (m, 5H). ^{13}C NMR (75 MHz, CD_3OD): δ 19.74, 103.62, 118.05, 121.72, 127.31, 130.11, 131.93, 132.06, 132.65, 134.31, 137.21, 161.11, 166.84, 173.47. MS (EI^+): m/z 302 (M^+). HRMS (ESI^+): m/z calcd for $(M + H)^+$, 303.10212; found, 303.10060.

9-[1-(2,4-Dimethylphenyl)]-6-hydroxy-3*H*-xanthen-3-one (2). Yield: 86%. ^{1}H NMR (300 MHz, CD_3OD): δ 2.01 (s, 3H), 2.49 (s, 3H), 7.19−7.26 (m, 3H), 7.32−7.39 (m, 4H), 7.60 (d, 2H, J = 9.2 Hz). ^{13}C NMR (75 MHz, CD_3OD): δ 19.74, 21.40, 103.52, 118.36, 121.53, 127.96, 129.62, 130.17, 132.72, 134.64, 137.10, 142.56, 161.23, 168.48, 173.04. MS (EI^+): m/z 316 (M^+). HRMS (ESI^+): m/z calcd for $(M + H)^+$, 317.11777; found, 317.11538.

9-[1-(2,5-Dimethylphenyl)]-6-hydroxy-3*H*-xanthen-3-one (3). Yield: 89%. ^{1}H NMR (300 MHz, CD_3OD): δ 1.99 (s, 3H), 2.42 (s, 3H), 7.13 (s, 1H), 7.19 (dd, 2H, J = 2.4, 9.2 Hz), 7.30 (d, 2H, J = 2.2 Hz), 7.43 (s, 2H), 7.54 (d, 2H, J = 9.4 Hz). ^{13}C NMR (75 MHz, CD_3OD): δ 19.21, 20.90, 103.62, 118.01, 121.72, 130.40, 131.97, 132.54, 132.60, 134.06, 134.37, 137.37, 161.05, 166.90, 173.53. MS (EI^+): m/z 316 (M^+). HRMS (ESI^+): m/z calcd for $(M + H)^+$, 317.11777; found, 317.11472.

9-[1-(2-Methoxyphenyl)]-6-hydroxy-3*H*-xanthen-3-one (4). Yield: 91%. ^{1}H NMR (300 MHz, CD_3OD): δ 3.74 (s, 3H), 7.20−7.38 (m, 7H), 7.67−7.77 (m, 3H). ^{13}C NMR (75 MHz, CD_3OD): δ 56.36, 103.33, 113.18, 118.37, 121.28, 122.07, 131.87, 134.24, 134.95, 158.00, 161.15, 166.44, 172.81. MS (EI^+): m/z 318 (M^+). HRMS (ESI^+): m/z calcd for $(M + H)^+$, 319.09703; found, 319.09433.

9-[1-(2-Methyl-4-methoxyphenyl)]-6-hydroxy-3*H*-xanthen-3-one (5). Yield: 89%. ^{1}H NMR (300 MHz, CD_3OD): δ 2.03 (s, 3H), 3.93 (s, 3H), 7.06 (dd, 1H, J = 2.2, 8.4 Hz), 7.11 (d, 1H, J = 2.0 Hz), 7.21 (dd, 2H, J = 2.2, 9.2 Hz), 7.24 (d, 1H, J = 7.5 Hz), 7.32 (d, 2H, J = 2.2 Hz), 7.61 (d, 2H, J = 9.3 Hz). ^{13}C NMR (75 MHz, CD_3OD): δ 20.16, 56.02, 103.56, 112.97, 117.38, 118.49, 121.54, 124.60, 131.90, 134.61, 139.24, 161.07, 163.19, 167.58, 173.20. MS (EI^+): m/z 332 (M^+). HRMS (ESI^+): m/z calcd for $(M + H)^+$, 333.11268; found, 333.10856.

9-[1-(2-Methoxy-5-methylphenyl)]-6-hydroxy-3*H*-xanthen-3-one (6). Yield: 87%. ^{1}H NMR (300 MHz, CD_3OD): δ 2.40 (s, 3H), 3.70 (s, 3H), 7.17 (d, 1H, J = 1.8 Hz), 7.24 (dd, 2H, J = 2.2, 9.2 Hz), 7.25 (d, 1H, J = 8.6 Hz), 7.35 (d, 2H, J = 2.2 Hz), 7.54 (dd, 1H, J = 2.2, 8.6 Hz), 7.72 (d, 2H, J = 9.2 Hz). ^{13}C NMR (75 MHz, CD_3OD): δ 20.39, 56.36, 103.29, 113.07, 118.36, 121.03, 121.23, 131.86, 132.07, 134.57, 135.05, 155.93, 161.11, 166.65, 172.77. MS (EI^+): m/z 332 (M^+). HRMS (ESI^+): m/z calcd for $(M + H)^+$, 333.11268; found, 333.10945.

9-[1-(2,4-Dimethoxyphenyl)]-6-hydroxy-3*H*-xanthen-3-one (7). Yield: 89%. ^{1}H NMR (300 MHz, CD_3OD): δ 3.74 (s, 3H), 3.97 (s, 3H), 6.86 (dd, 1H, J = 2.2, 8.4 Hz), 6.89 (d, 1H, J = 2.0 Hz), 7.23 (dd, 2H, J = 2.2, 9.2 Hz), 7.29 (d, 1H, J = 8.8 Hz), 7.31 (d, 2H, J = 2.2 Hz), 7.77 (d, 2H, J = 9.2 Hz). ^{13}C NMR (75 MHz, CD_3OD): δ 56.35, 56.36, 100.16, 103.26, 107.11, 113.62, 118.48, 121.03, 133.47, 135.22, 159.58, 161.02, 165.72, 166.39, 172.57. MS (EI^+): m/z 348 (M^+). HRMS (ESI^+): m/z calcd for $(M + H)^+$, 349.10760; found, 349.10457.

9-[1-(2,5-Dimethoxyphenyl)]-6-hydroxy-3*H*-xanthen-3-one (8). Yield: 85%. ^{1}H NMR (300 MHz, CD_3OD): δ 3.68 (s, 3H), 3.82 (s, 3H), 6.97 (d, 1H, J = 1.8 Hz), 7.26 (dd, 2H, J = 2.4, 9.2 Hz), 7.29 (m, 2H), 7.37 (d, 2H, J = 2.4 Hz), 7.74 (d, 2H, J = 9.2 Hz). ^{13}C NMR (75 MHz, CD_3OD): δ 56.45, 56.70, 103.29, 114.35, 117.44, 118.35, 118.87, 121.31, 121.75, 135.02, 151.87, 155.22, 161.20, 166.20, 172.79. MS (EI^+): m/z 348 (M^+). HRMS (ESI^+): m/z calcd for $(M + H)^+$, 349.10760; found, 349.10382.

Preparation of 2-Me-4-MeO TokyoGreen Mono(2′,3′,4′,6′-tetra-*O*-acetyl-*β*-D-galactopyranoside) (TG-*β*Gal Tetraacetate). A mixture of 2-Me-4-OMe TokyoGreen (**5**) (10 mg, 30 μmol), Cs_2CO_3 (100 mg, 300 μmol), and 2,3,4,6-tetra-*O*-acetyl-α-D-galactopyranosyl bromide (100 mg, 250 μmol) in dry dimethylformamide (0.5 mL) was stirred overnight at room temperature under Ar. The inorganic precipitate was filtered off, and the filtrate was concentrated under reduced pressure. The residue was diluted with water and extracted with CH_2Cl_2 three times. The combined organic solution was washed with water and saturated NaCl(aq), dried over Na_2SO_4, and evaporated. The residue was chromatographed on silica gel with CH_2Cl_2−MeOH (100:3) as the eluent to give TG-*β*Gal tetraacetate (11.3 mg, 57%) as an orange powder. ^{1}H NMR (300 MHz, $CDCl_3$): δ 2.03 (s, 3H), 2.05 (s, 3H), 2.07 (s, 3H), 2.14 (s, 3H), 2.20 (s, 3H), 3.90 (s, 3H), 4.10−4.25 (m, 3H), 5.12−5.19 (m,2H), 5.48−5.58 (m, 2H), 6.40 (d, 1H, J = 1.4 Hz), 6.57 (dd, 1H, J = 1.4, 9.3 Hz), 6.80−7.11 (m, 7H). HRMS (ESI^+): m/z calcd for $(M + Na)^+$, 685.18971; found, 685.18920.

Preparation of 2-Me-4-MeO TokyoGreen Mono-*β*-D-galactopyranoside (TG-*β*Gal). To a solution containing 34 mg (51.3 μmol) of 2-Me-4-OMe TokyoGreen mono(2′,3′,4′,6′-tetra-*O*-acetyl-*β*-D-galactopyranoside) in 2 mL of methanol was added 10.5 μL of 4.9 M NaOMe (51.3 μmol). After being stirred at 0 °C for 30 min, the reaction mixture was neutralized with Amberlite IR-120 plus (H^+). The Amberlite was filtered off, and the filtrate was evaporated. The obtained residue was chromatographed on reversed-phase preparative TLC (RP18W) with CH_3CN−H_2O (1:1) as the eluent to give 2-Me-4-OMe TokyoGreen mono-*β*-D-galactopyranoside (21.7 mg, 85.4%) as an orange powder. ^{1}H NMR(300 MHz, CD_3OD): 2.03 (s, 3H), 3.61 (dd, 1H, J = 3.4, 9.5 Hz), 3.74−3.88 (m, 4H), 3.89 (s, 3H), 3.92 (d, 1H, J = 3.9 Hz), 5.10 (dd, 1H, J = 2.8, 7.9 Hz), 6.47 (d, 1H, J = 2.0 Hz), 6.62 (dd, 1H, J = 2.0, 9.5 Hz), 7.00−7.21 (m, 6H), 7.37 (d, 1H, J = 2.4 Hz). HRMS (ESI^+): m/z calcd for $(M + Na)^+$, 517.14745; found, 517.15056.

Fluorescence Properties and Quantum Efficiency of Fluorescence. Steady-state fluorescence spectroscopic studies were performed on an F4500 (Hitachi). UV−vis spectra were obtained on a UV-1600 (Shimadzu), with 0.1 mol L^{-1} sodium phosphate buffer (pH 3.4) or NaOH(aq) (pH 13) as the solvent. Each solution contained up to 0.1% (v/v) DMSO as a cosolvent. For determination of the quantum efficiency of fluorescence (Φ_{fl}), fluorescein in 0.1 mol L^{-1} NaOH(aq) (Φ_{fl} = 0.85) was used as a fluorescence standard.[6] Curve fittings in Figure 2b,c were done by the Marcus[17] and Rehm−Weller[18] equation with the constant values of λ = 0.81 eV, $k_f = 2.01 \times 10^8$ s^{-1}, Φ_{fl} = 0.85 for the anion form of fluorescein, and Φ_{fl} = 0.32 for the neutral form of fluorescein and with w_p and V values as variables.[13]

Cyclic Voltammetry. Cyclic voltammetry was performed on a 600A electrochemical analyzer (ALS). A three-electrode arrangement in a single cell was used for the measurements: a Pt wire as the auxiliary electrode, a glassy carbon electrode as the working electrode, and a Ag/Ag^+ electrode as the reference electrode. The sample solutions contained 1.0×10^{-3} M sample and 0.1 M tetrabutylammo-

nium perchlorate (TBAP) as a supporting electrolyte in acetonitrile, and argon was bubbled for 10 min before each measurement. Obtained potentials (vs Ag/Ag^+) were converted to those vs SCE by adding 0.248 V.

***β*-Galactosidase Assay.** TG-*β*Gal and FDG were dissolved in anhydrous DMSO to obtain 100 mM stock solutions. Both probes were diluted with buffer (specified below for in vitro enzymatic experiments and in the next section for fluorescence imaging in cells) to the desired concentration. For in vitro enzymatic experiments, both probes were used at a final concentration of 1.0 μM. All fluorescence measurements and enzymatic reactions of β-galactosidase were performed at 37 °C in a 3 mL total volume of 100 mM sodium phosphate buffer, pH 7.4, containing 14.3 mM 2-mercaptoethanol, 1 mM $MgCl_2$, 0.1% DMSO, and 6 U of β-galactosidase in a 1 cm cuvette. Fluorescence spectral changes of the two probes were measured with a Perkin-Elmer LS-50B fluorescence spectrometer. The excitation wavelength was 490 nm, and the emission wavelength was 510 nm for TG-*β*Gal and 513 nm for FDG.

Fluorescence Imaging in Cells. For fluorescence imaging in cells, TG-*β*Gal and FDG were used at a final concentration of 10 μM in physiological salt solution, pH 7.4, containing 150 mM NaCl, 4 mM KCl, 2 mM $CaCl_2$, 1 mM $MgCl_2$, 5 mM HERES, and 0.1% glucose (PSS). GP293 cells transduced with LNCX2-*lacZ* (*lacZ*-positive cells) were seeded onto a collagen type I-coated 24-well microplate. Cells were washed with PSS twice and then loaded with TG-*β*Gal or FDG dissolved in PSS by incubation for 30 min at room temperature. GP293 cells (*lacZ*-negative cells) were also used as negative controls. Confocal fluorescence images were captured using an Olympus fluoview system using an IX81 inverted microscope, an Ar ion laser, and a PlanApo 60×/1.40 objective lens (Olympus, Tokyo, Japan). The excitation wavelength was 488 nm, and the emission wavelength was 510−550 nm.

Acknowledgment. This study was supported in part by a grant for the Precursory Research for Embryonic Sciences and Technology from the JST Agency to Y.U., a Grant-in-Aid for Creative Scientific Research (No. 13NP0401), research grants (Grant Nos. 12771349, 13557209, 14103018, 16651106, and 16689002 to Y.U.), and a grant for the Advanced and Innovational Research Program in Life Sciences to T.N. from the Ministry of Education, Culture, Sports, Science and Technology of the Japanese Government and by a grant from the Kowa Life Science Foundation to Y.U.

JA043919H